A Locally-Preferred Structure Characterizes All Dynamical Regimes of a Supercooled Liquid

Ryan Soklaski,[1] Vy Tran,[1] Zohar Nussinov,[1,2] K.F. Kelton,[1] and Li Yang[1]

[1]*Department of Physics and Institute of Materials Science and Engineering,*

Washington University in St. Louis, St. Louis, MO 63130, USA

[2]*Department of Condensed Matter Physics,*

Weizmann Institute of Science, Rehovot, 76100 Israel

(Dated:)

Abstract

Recent experimental results suggest that metallic liquids universally exhibit a high-temperature dynamical crossover, which is correlated with the glass transition temperature (T_g). We demonstrate, using molecular dynamics results for $Cu_{64}Zr_{36}$, that this temperature, $T_A \approx 2 \times T_g$, is linked with cooperative atomic rearrangements that produce domains of connected icosahedra. Supercooling to a new characteristic temperature, T_D, is shown to produce higher-order cooperative rearrangements amongst connected icosahedra, which manifests as the formation of large Zr-rich connected domains that possess macroscopic proportions of the liquid's icosahedra. This coincides with the decoupling of atomic diffusivities, large-scale domain fluctuations, and the onset of glassy dynamics in the liquid. These extensive domains then abruptly stabilize above T_g and eventually percolate before the glass is formed. All characteristic temperatures (T_A, T_D and T_g) are thus connected by successive manifestations of the structural cooperativity that begins at T_A.

PACS numbers:

INTRODUCTION

As a liquid is supercooled below its melting temperature, the characteristic timescales of its dynamics become increasingly stretched. In a dramatic departure from exhibiting simple diffusive particle dynamics, its viscosity, η, increases rapidly as it develops general, glassy dynamic features [1–4]. Efforts to universally describe these phenomena as a liquid is supercooled to its glass transition temperature (T_g) remain divided in both their approaches and successes [3–13]. In these theories, the roles played by structure, if any, are a major point of discrepancy. The molecular dynamics (MD) results presented here reveal a striking correlation between structure and dynamics across a broad temperature range. In particular, a high temperature structural crossover is shown to underlay a recently reported dynamical one [14].

Numerous works point to the fundamental importance of locally-preferred structures (LPS)s in glass forming liquids [13, 15–18]. One such thermodynamic theory describes the growth of frustration-limited domains (FLD)s of the LPS as the liquid is cooled [13, 19, 20]. This FLD theory accurately describes glassy relaxation processes and predicts a temperature, T_A, below which a fragile liquid develops a super-Arrhenius temperature dependence for η. Very recently, an analysis of experimental data for a wide variety of metallic liquids revealed that T_A correlates strongly with T_g, such that $T_A \approx 2 \times T_g$ [14]. This temperature may correspond to a crossover phenomenon created by competition between configurational excitations and phonons [21]. Remarkably, it was found that, by using T_A and particle density as scaling factors, the viscosity data for all strong and fragile metallic liquids fall on a universal curve across a broad temperature range [14, 19].

Despite the merits of the FLD theories, an important problem persists. The measured structural changes of the liquid across the accessible supercooled temperature range are extremely subtle, casting doubts on the extent and even the existence of the FLDs [3, 7] as well as the structural changes that accompany processes at T_A [15, 21]. Therefore, observing FLDs and studying their role in the dynamical crossover at T_A would bolster FLD theory, the interpretation of the apparent universality across metallic liquids, and the overall understanding of the relationship between structure and dynamics in liquids

In this work, we demonstrate the development and growth of FLDs in a metallic liquid as it is cooled through T_A, providing a coherent picture of the structural and dynamical

features of the cooperativity that arises at this crossover temperature as well as within the supercooled regime. Rapidly growing fluctuations in domain sizes are linked to the development of glassy dynamics, leading to the identification of another crossover at lower temperature, T_D, which may be possible to observe in experimental structural studies [22, 23]. While supercooling, these extensive domain then quickly stabilize, marked by a sudden drop in domain fluctuations, and percolate across the system before the temperature reaches T_g. The MD results presented here suggest that all of these characteristic temperatures, T_A, T_D and T_g correspond to a cascade of cooperative structural rearrangements involving a LPS that begins at T_A, a result consistent with the prediction from recent experimental studies of viscosity [14].

The remainder of this paper is organized as follows: in section II, we introduce the methods of our MD simulations. In section III, we discuss our methods of our Voronoi analysis, and introduce definitions of icosahedral ordering. Section IV introduces the temperatures T_A and T_D, and the dynamical features that accompany them. Section V defines liquid relaxation and restructuring timescales and discusses the role played by cooperative structural rearrangements at T_A and T_D. Here also we show that T_A marks the onset of connected icosahedral ordering. Section VI links that dynamical features that begin at T_D with the rapid proliferation of connected domains of icosahedra. Section VII provides an overview of the structure-dynamic relationships of the liquid and its icosahedron domains from high temperatures down to T_g, where were find that a single domain of icosahedra has percolated the system. Section VIII contains a summary of our findings.

METHODS

Results were obtained from classical MD simulations of the metallic liquid $Cu_{64}Zr_{36}$, which among best glass forming compositions of this alloy [24]. All MD simulations were conducted using LAMMPS [25] with GPU-parallelization packages [26]. Atomic interactions in the $Cu_{64}Zr_{36}$ system, including approximations of many-body interactions, are described using the Finnis-Sinclair generalization of the embedded atom method [27]. This semi empirical potential was selected for its ability to accurately reproduce structures and properties of $Cu_{64}Zr_{36}$ in both the liquid and glass regimes, as confirmed by comparisons made with x-ray diffraction data and ab initio calculation results [28]. The reported calorimetric glass

formation temperature (T_g) for this potential is approximately $750K$. We confirm this by measuring the system volume, given zero average pressure, as a function of temperature, and identifying the temperature at which the thermal expansion coefficient changes.

Isothermal, isobaric simulations (sampled from ensembles with constant N, $\langle P \rangle$, and $\langle T \rangle$ [29]) were conducted with $\langle P \rangle = 0$ and $N = 3 \times 10^4$ atoms, using periodic boundary conditions, the Verlet integration method, and the Nose-Hoover thermostatting method. Each simulation was initialized with a random atomic configuration that evolves at $T = 3300K$ for $0.5ns$ to achieve equilibrium. The liquid was then quenched at a rate of $10^{11} K/s$ down to its target temperature and subsequently relaxed for $20ns$ before structure and dynamics data were collected. The integration timestep during the quenching and relaxation processes was $5fs$. The integration step was then decreased to $2fs$, and data was collected for each timestep. For a given target temperature, atomic-level data, such as the positions and velocities were recorded across a $0.2ns$ interval; the system's Cauchy stress tensor was recorded for $8ns$. Additional independent simulations were conducted for all temperatures below $1100K$ in addition to $2200K$ and $2500K$. To check for system size effects, additional simulations of $N = 1 \times 10^4$ atoms were performed.

ICOSAHEDRAL ORDERING AND FRUSTRATION-LIMITED DOMAINS

Voronoi analysis utilizing a weighted-bisector method was performed utilizing the Voro++ software library [30]. Small faces comprising less than 0.5% of a Voronoi cell's surface area were removed. The analysis was performed on each time step for which atomic positions were recorded. The LPS for $Cu_{64}Zr_{36}$ is an icosahedron-shaped cluster of atoms [31–34], consisting of a Cu atom with 12 nearest neighbor atoms, which form a weighted-Voronoi cell with 12 pentagonal faces. Distorted icosahedra, which contain some non-pentagonal Voronoi faces, are treated as distinct structures and are not considered to be LPSs. FLDs are thus comprised of connected icosahedra. Two icosahedra are connected if they share a vertex, an edge, a face, or they interpenetrate, meaning that they share 1, 2, 3, or 7 atoms, respectively [35].
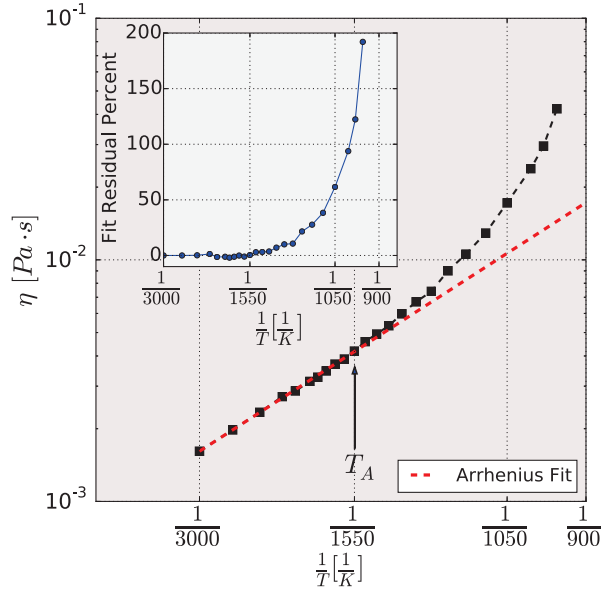
FIG. 1: (Color online) Viscosity, η, as a function of $\frac{1}{T}$. η begins to exhibit super-Arrhenius growth below $T_A = 1550K$. (Inset) The percent residual of η from the Arrhenius fit.

DYNAMICAL FEATURES OF LIQUID $Cu_{64}Zr_{36}$: BREAK DOWN OF STOKES-EINSTEIN AND DECOUPLING OF DIFFUSIVITIES

Before analyzing the structural evolution of $Cu_{64}Zr_{36}$, a summary of the dynamical features that develop in the liquid across a broad temperature range is presented. Viscosity (η) data obtained using the Green-Kubo relationship for the stress tensor autocorrelation function [36] are shown in the main panel of Figure 1. A change from an Arrhenius temperature dependence to a super-Arrhenius form occurs when the liquid is cooled below $1550K$, which is therefore identified as T_A. In accord with recent experimental study [14], this value is near $2 \times T_g$ ($T_g \approx 750K$ [28]).

The liquid diffusivity data, plotted in the inset of Figure 2, maintains an Arrhenius form through lower temperatures than does η, indicating that T_A also marks the breakdown of the Stokes-Einstein relationship for Zr atoms,

$$\eta \cdot D_{Zr} \propto \frac{k_B \cdot T}{R_{Zr}}, \tag{1}$$

which are the larger diffusing solute species in the system [3, 37]. Here, D_{Zr} is the diffusion coefficient of tagged Zr particles as measured from the long-time integral of their velocity autocorrelation functions, T is the temperature, and R_{Zr} is the effective particle radius. The
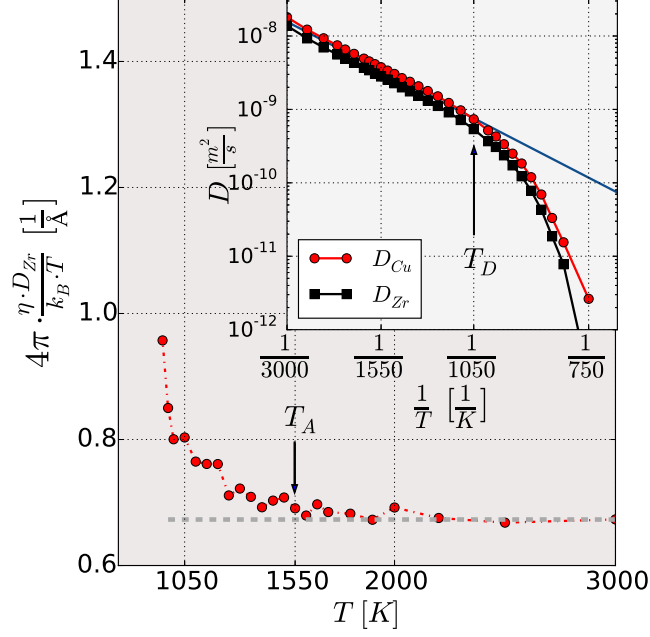
FIG. 2: (Color online) The Stokes-Einstein ratio as a function of T. The Stokes-Einstein relationship becomes violated below T_A (Inset) Cu and Zr diffusivities versus $\frac{1}{T}$. A transition from a high-T linear fit on a log scale (solid line) occurs at $T_D = 1050K$ for both species.

data presented in the main panel of Figure 2 shows that for high temperatures the Stokes-Einstein ratio is roughly a constant 0.67, which is comparable to $\frac{1}{R_{Zr}} \approx 0.65$ $1/\mathring{A}$ [38]. At T_A, the accelerated growth in η causes a deviation from this constant, indicating that the liquid is departing from its "simple" behavior, and is developing dynamical heterogeneities [6, 39]. Specifically, slow-moving regions develop in the liquid that dictate the timescale of structural relaxations, as measured by η, whereas fast-moving regions control the dynamical timescale proportional to $\frac{1}{D}$.

It is striking to find that the Stokes-Einstein relationship is violated at such a high temperature - literature reviews of supercooled liquids broadly indicate that this relationship is expected to hold well into a liquid's supercooled regime [3, 8]. However, this prescription is chiefly informed by empirical studies of molecular liquids, such as o-terphenyl, where the violation occurs near $1.2 \times T_g$ (near the mode-couple temperature) [40, 41]. Our finding, that the Stokes-Einstein relationship is violated well above $1.2 \times T_g$, are supported by several empirical studies of metallic liquids [42–44]. Furthermore, an illuminating concurrent MD study of liquid $Cu_{40}Zr_{51}Al_9$ submitted very shortly after the original submission of the
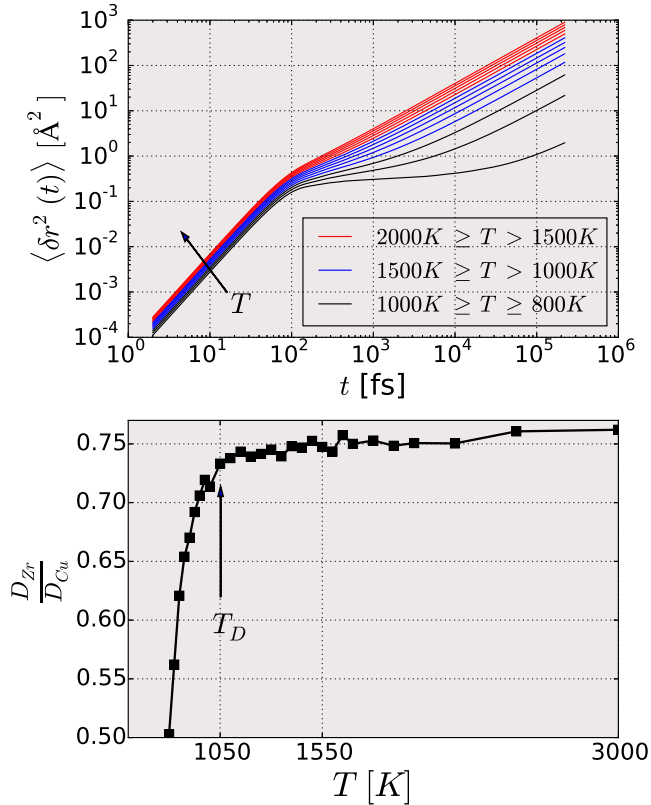
FIG. 3: (Color online) (Top) The mean-squared displacement time-trajectories of atoms for various liquid temperatures on a log-log scale. The temperatures included are separated by $100K$ intervals. A distinct plateau feature, characteristic of glassy dynamics, develops for $T \lesssim T_D$. (Bottom) The ratio of the diffusivity of Zr atoms to that of Cu atoms. The diffusivities are found to decouple sharply for $T \leq T_D$.

current work similarly found that the relation breaks down specifically at $T_A \approx 2 \times T_g$ for that alloy as well [45]. Taken together, these results bolster our finding of Stokes-Einstein violation at T_A to a broader range of materials

It is important to note that the local violation of the Stokes-Einstein equation at T_A does not signify the onset of strong glassy dynamics in $Cu_{64}Zr_{36}$. That is, the system does not yet exhibit plateau-separated fast (β) and slow (α) relaxation processes at T_A. This can be seen in the inset of Figure 2, which displays the temperature dependence of the diffusivities for Cu and Zr particles, and in the top panel of Figure 3, which contains a series of mean-squared displacement (MSD) time trajectories for several temperatures. The MSD trajectory at T_A exhibits an immediate transition between simple ballistic and diffusive

motion regimes without any plateau feature. This changes once the diffusivity, $D(T)$, departs from an exponentially-decaying function of $1/T$ at $1050K$, which we label T_D. D reflects the long-time asymptotic behaviors of the particles' MSDs: $\langle \delta r(t)^2 \rangle \sim 6Dt$ $(t \to \infty)$, thus the accelerated decline in $D(T)$ for both atomic species reflects the development of a sustained plateau that separates two-step relaxation processes in the supercooled liquid (Fig 3), as well as growing diffusive-motion activation energy barriers. This is characteristic of caged particle dynamics and is an important equilibrium signature of the impending glass transition [3, 4].

Also at T_D, the motions of Cu and Zr atoms begin to decouple, leading to a sharp decrease in $\frac{D_{Zr}}{D_{Cu}}$ with decreasing temperature; this is shown in the lower panel of Figure 3. Here, the system's energy landscape begins to to disproportionately impede the activation of the larger Zr atoms, whereas above T_D, the two species diffuse via the same physical mechanism with $\frac{D_{Zr}}{D_{Cu}} \approx \frac{R_{Cu}}{R_{Zr}}$ [38]. This decoupling strongly suggests that a structural feature begins to emerge at T_D that skews the supercooled liquid's dynamics. We will investigate this underlying structure in section VI. Lastly, we note that a recent empirical study of a Zr-based metallic liquid reports a similar decoupling of dynamics at a temperature comparable to T_D [46].

In summary, T_A $(1550K)$ is the temperature below which η begins to exhibit super-Arrhenius growth, and where the Stokes-Einstein relationship first breaks down in the liquid. T_D $(1050K)$ then marks the early onset of stretched, glassy dynamical features in the supercooled liquid, which appear to be shaped by an emerging robust structural feature.

T_A AND COOPERATIVE STRUCTURAL REARRANGEMENTS

The crossover from the "simple liquid" regime at T_A marked by the development of super-Arrhenius relaxation times, and the development of glassy dynamics at T_D both coincide with the onset of structural cooperativity associated with FLDs of connected icosahedra. Our analysis of this cooperativity follows and expands on the work of Iwashita, Nicholson, and Egami [21] and introduces three pertinent timescales. First, the Maxwell time, or shear stress relaxation time,

$$\tau_M \equiv \frac{\int_0^\infty \langle \sigma_{ij}(t)\sigma_{ij}(0)\rangle dt}{\langle \sigma_{ij}(0)^2 \rangle}, \tag{2}$$

provides a timescale during which the liquid behaves like a solid and exhibits an elastic shear response without flowing [3, 37]. $\sigma_{ij}(t)$ is the time-dependent Cauchy stress tensor [37]. Second, the local cluster time, τ_{LC}, is defined as the average time required for an
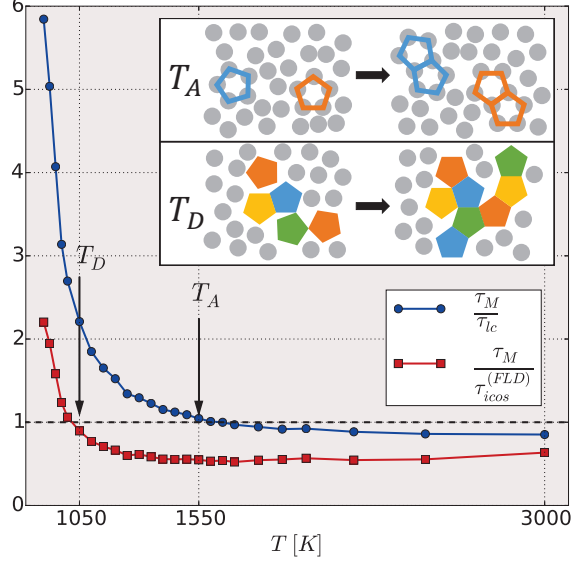
FIG. 4: (Color online) Ratio of the Maxwell time to the local cluster time and the domain-connected icosahedron lifetime, respectively. τ_M surpasses τ_{LC} and $\tau_{icos}^{(FLD)}$ at T_A and T_D, respectively. (Inset) A 2D illustration of the cooperative rearrangements that begin contributing to the liquid relaxation process at T_A and at T_D, respectively. Here the 2D pentagons represent 3D icosahedral clusters of atoms.

atom to change its coordination number, i.e. the time needed for an atom to lose or gain a Voronoi neighbor. In addition to these two times, we introduce the icosahedron lifetime, τ_{icos}, which is the average time required for an icosahedron to lose a vertex atom, gain an extraneous vertex atom, or distort its shape. τ_{icos} for an icosahedron involved in a domain via interpenetrating connection is labelled $\tau_{icos}^{(FLD)}$. Measurements of τ_{LC} and τ_{icos} provide a context for understanding the timescales over which atomic rearrangements of the liquid structure occur.

The primary portion of Figure 4 shows the ratios of τ_M to τ_{LC} and $\tau_{icos}^{(FLD)}$, respectively, as a function of temperature. Liquid relaxation in the high temperature, simple liquid regime ($T > T_A$) is characterized by uncorrelated local rearrangements of atomic clusters: $\tau_M \approx \tau_{LC}$. That the high temperature liquid relaxation time is generally controlled by τ_{LC} in atomic liquids was first shown by Iwashita *et al.* [21]. Here, τ_M is so short that consecutive atomic rearrangements occur only after the surrounding environment has relaxed in response to shear strains. It is not until the system is cooled through T_A that $\tau_M > \tau_{LC}$, and that typical atomic clusters can begin to rearrange with one another on a time scale during which
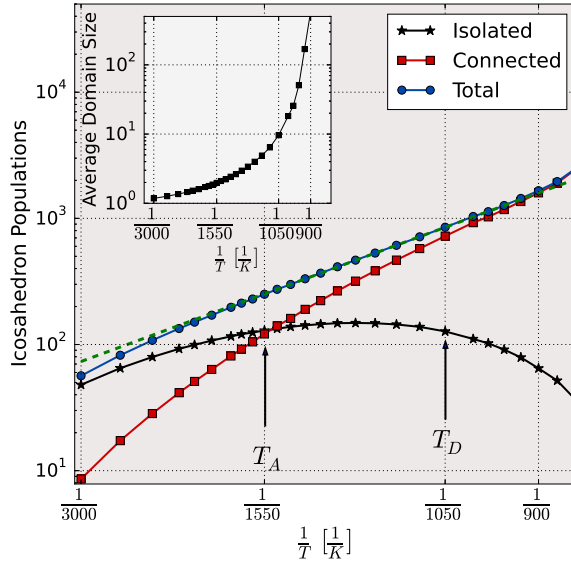
9

FIG. 5: (Color online) The populations of connected and isolated icosahedra, plus their sum. A low-T linear fit on the log scale is indicated with a dashed line. A crossover in the isolated and connected populations occurs as the liquid is cooled throug T_A. (Inset) The average connected-icosahedron domain size, $\bar{s}$, on a log scale. A domain's size is given by the number of icosahedra participating in a singly-connected structure

the liquid behaves like a solid. Here cooperative restructuring can begin contributing to the liquid's relaxation process [21].

What is produced by these cooperative rearrangments? That is, what difference is there between the average structure of the liquid at temperatures above T_A and those below? Measuring the the populations of the isolated, and connected icosahedra in a volume containing 3×10^4 atoms reveals that a structural crossover occurs at T_A: above T_A it is more likely to find isolated icosahedra than connected ones, and below T_A connected icosahedra become the dominant population. This can be seen in Figure 5, which shows, on a log scale, the evolution of these icosahedron populations as well as the total number of icosahedra. The total population of icosahedra proceeds to grow exponentially with inverse temperature for $T_A > T$. In the context of our timescales, we find that in the regime where $T_A > T > T_D$ icosahedra are stable in comparison to the average local cluster configuration ($\tau_{icos}^{FLD} > \tau_{LC}$), and are relatively robust on the timescale of liquid relaxation ($\tau_{icos}^{FLD} \gtrsim \tau_M$) across this temperature range. Thus the liquid relaxation process chiefly involve non-icosahedral atomic
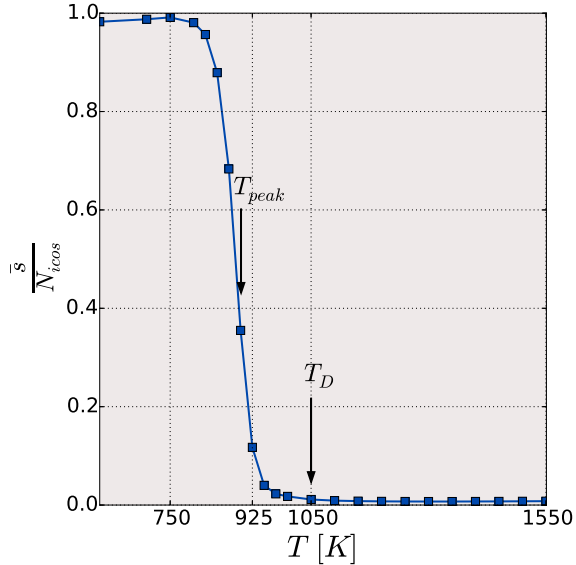
10

FIG. 6: (Color online) The fraction of the total number of icosahedra in a 30,000 atom system, N_{icos}, contained in an FLD. Below T_D, a domain contains a macroscopic number of the system's icosahedra. T_{peak} marks the maximum susceptibility of the fractional occupation.

clusters, which cooperatively rearrange amidst the relatively inert icosahedra and form off of them, new, connected icosahedra. This process is depicted in a simplified 2D illustration in the inset of Figure 4.

It is quite remarkable that the distinct dynamical features associated with T_A are linked with the incipient icosahedral ordering in this system. While the structure-dynamics features of icosahedron networks are becoming well-documented for temperatures near T_g [32, 33, 47], the roles played by these structures at higher temperatures have remained largely unknown. Thus our findings stand amongst the first explicit accounts of the structural features that accompany the emergence of solidlike features in high temperature metallics liquids. They also correspond closely with the narrative of FLD theory, which predicts the development of frustrated domains at T_A in association with an avoided critical point in the system [13, 19, 20]. We proceed by further tracking this icosahedral ordering into the supercooled region, where prominent structural features are expected to emerge near T_D.
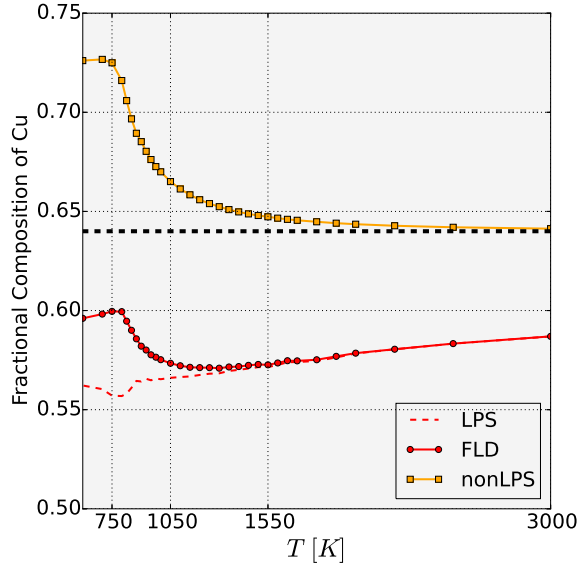
FIG. 7: The concentration of Cu atoms in: an average 13-atom icosahedron (red dashed-line), the connected icosahedron domains (red circles), and in non-icosahedron structures (yellow squares). When approaching T_g, the preferential sharing of Zr atoms amongst icosahedra allows the extensive FLDs to approach the overall alloy composition, while preserving the Zr-rich environment required by the icosahedra.

T_D AND THE RAPID ONSET OF DOMINANT ICOSAHEDRAL ORDERING

As the liquid is supercooled through T_D, its relaxation time grows such that $\tau_M \gg \tau_{icos}^{(FLD)}$ for $T < T_D$ (see Fig 4), and thus its relaxation processes begin to involve consecutive structural rearrangements of connected icosahedra within FLDs. The illustration in Figure 4 depicts a simple schematic of such processes. We find that the onset of this medium-ranged cooperative restructuring accompanies the enhancement of the diffusive-motion energy barrier and the early development of general glassy dynamics observed at T_D, and it leads to a dramatic proliferation of highly connected FLDs of icosahedra throughout the liquid.

The size of an FLD is measured by the number of icosahedra participating in the connected domain. The inset of Figure 5 shows the the weighted average FLD size, $\bar{s}$, whose growth accelerates tremendously with decreasing temperature - note that the data is plotted on a log scale. The fractional occupation of an average FLD - the proportion of the icosahedron population in a 30,000 atom system contained in a typical connected domain - is plotted in Figure 6 versus inverse temperature. Here we see that cooling through T_D leads

12

to a dramatic unification of the liquid's FLDs. Above T_D a typical FLD contains a neglible portion of all the icosahedra, whereas below T_D the rapidly growing FLDs begin join with one another, such that macroscopic number of the system's icosahedra can be found in a single connected FLD. The peak value in the susceptibility of the fractional occupation number, $\frac{d}{dT}(\bar{s}/N_{icos})$, resides near $900K$ and is marked T_{peak}. By $825K$, $\bar{s}/N_{icos}$ nearly reaches unity - only a negligible number of icosahedra can be found to be separate from a single, extensive network of icosahedra.

These extensive FLDs, we propose, are the underlying structures responsible for the decoupled dynamics and the enhanced barriers to diffusion that emerge below T_D. Indeed, the disproportionately depressed diffusivity for Zr can be accounted for by considering the chemical ordering that accompanies the formation of FLDs. In accordance with efficient packing schemes of different-sized hard spheres [34, 48], icosahedra are Zr-rich relative to the overall alloy composition $Cu_{64}Zr_{36}$ - below T_A an icosahedron has an approximate composition of $Cu_{57}Zr_{43}$. An earlier MD study showed that non-interpenetrating connections between the icosahedra in an FLD strongly favor sharing Zr atoms amongst one another [35]; for instance, 80% of all shared vertices are Zr atoms, whereas the icosahedron shell composition is only 43% Zr. Thus non-interpenetrating connections within FLDs are utilized to foster a locally Zr-rich environment for the icosahedra, while the FLDs at large can, necessarily, maintain a composition closer to that of the alloy. The temperature dependent Cu concentrations of individual icosahedra (including the center Cu atoms), FLDs, and the non-icosahedron regions of the liquid are plotted in Figure 7.

There are numerous studies that demonstrate the unique role played by icosahedron FLDs in creating strong dynamical heterogeneities in $Cu_{64}Zr_{36}$ as it is supercooled towards T_g [32, 33, 47]. In particular, Y. Zhang *et al.* recently showed quite explicitly that diffusing atoms strongly avoid regions of icosahedral ordering, and that they instead reside in liquidlike regions of the system [47]. They demonstrate that underlying the development of medium-ranged icosahedral ordering and glassy dynamics is a crucial correspondence between dynamical and structural correlation length scales in the liquid. We thus conclude that the growing barrier to diffusion and decoupled motions of Cu and Zr atoms, which ensue below T_D, is created by the rapidly proliferating, Zr-rich FLDs of connected icosahedra that form amidst Cu-rich liquidlike regions in the system.
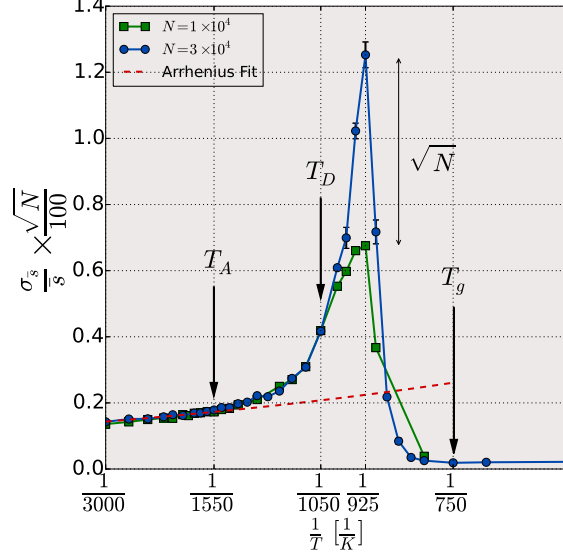
FIG. 8: Relative fluctuations of the mean connected-icosahedron domain size over time, as a function of $\frac{1}{T}$, scaled by $\sqrt{N}$, where N is the number of atoms in the system. A deviation from the high temperature Arrhenius fit (dashed curve) begins at T_A. Domain-size fluctuations grow rapidly upon cooling through T_D, and become system size independent. The distinct peak near $925K$ demonstrates the abrupt stabilization and growth of a large FLD, which percolates above T_g. Error bars are derived from averaging two independent runs

FLD FLUCTUATIONS AND FALLING OUT OF EQUILIBRIUM

Both cooperative characteristic temperatures, T_A and T_D, manifest as enhancements in fluctuations of the average domain size, $\overline{s}$. Figure 8 shows the relative time-fluctuations in domain size, $\frac{\sigma_{\overline{s}}}{\overline{s}}$, versus inverse temperature for system sizes of 1×10^4 and 3×10^4 atoms. The fluctuations are scaled by a factor of $\sqrt{N}/100$ to make-clear the behavior of system size effects. Here, $\overline{s}(t)$ is the mean domain size of the system at a time t, and $\sigma_{\overline{s}}$ is the standard deviation of $\overline{s}(t)$ from its time-averaged value, $\overline{s}$. As the liquid is cooled through T_A, fluctuations in the domain size become enhanced, growing faster than does the high-temperature Arrhenius fit (dashed curve) with decreasing temperature. Above T_D, the scaled fluctuations for the two system sizes collapse onto a single curve, indicating that FLD fluctuations scale as $\sim 1/\sqrt{N}$ in this temperature range. Cooling further through T_D leads to a breakdown in this scaling law, with the peak fluctuations growing as $\sim \sqrt{N}$ on the scaled axis - that is, the peak-value fluctuations appear to become system size independent.

14

By $T = 925K$ the cooperatively-rearranging FLDs attempt to grow far beyond their average sizes before inevitably collapsing, reaching relative fluctuations of 70%.

This behavior changes abruptly as the liquid is supercooled through $925K$. Here the FLDs begin to stabilize and the fluctuations in FLD size drop rapidly with decreasing temperature. We must consider whether this drop in fluctuations is actually a mark of structural stabilization or if it is a mere consequence of our simulation timescale becoming insufficient for capturing metasable equilibrium dynamics. It is certainly true that the fluctuations must inevitably fall to zero as we approach T_g given that τ_M will far outgrow our simulation timescale. That being said, τ_M is still sufficiently short at $900K$, where the fluctuations have already started to fall, that our liquid has been allowed to evolve for a time four orders of magnitude longer than the liquid relaxation time, and our data collection window is two orders of magnitude longer. Furthermore, several studies show that utilizing slower quench rates, longer relaxation time, and thermalization techniques only further enhances the degree of icosahedral ordering and the connectivity of the resulting FLDs [33, 47]. This indicates that the drop in fluctuations indeed reflects pronounced stabilization of the FLDs, and that the fluctuations in the extensive FLD's size would approach zero even if we were able to remain in equilibrium near T_g. By $900K$, nearly 40% of the system's icosahedra; as we saw in Figure 6, this fraction continues to grow rapidly until a single FLD percolates the system by $825K$ [35], where the fluctuations nearly reach zero. A structure is said to percolate a material when a singly-connected domain of that structure spans the material (e.g. a connected domain of icosahedra is as long as the diagonal length of our simulation box). Below T_g, the percolated FLD shapes the properties, mechanical and others, of the glass. This has been demonstrated by a number of excellent studies for several glasses [17, 49–54]. Not discussed in this paper are the roles played by the various types of connections that can form between icosahedra. For detailed discussions of this important aspect of icosahedral ordering, we refer the reader to early studies of this subject [33, 35].

In the limit of large system size, the peaked fluctuations in Figure 8 resembles closely the susceptibility of the fractional occupation plotted in Figure 6. We note that this and other features of the rapid development of extensive icosahedral ordering in this system indicates the possible presence of a liquid-liquid phase transition above T_g [11]. This will be investigated in detail in a future publication.

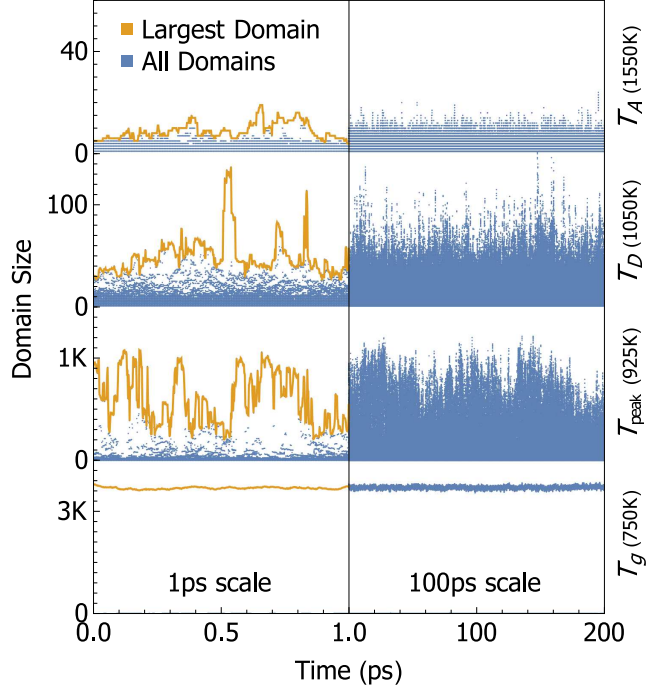Lastly, the time-dependent behavior of the FLDs that produce the fluctuations reported

FIG. 9: (Color Online) The connected-icosahedron domain sizes present at a given simulation time step plotted versus time. System temperatures are indicated on the right side of the plots. On the $1ps$ timescale, an orange trajectory traces the evolution of the largest domain size.

in Figure 8 are shown in Figure 9. Here, we plot all of the domain sizes that are present at each simulation time step, for temperatures T_A, T_D, T_{peak}, and T_g. The left side and right sides of the plot show this time dependence on $1ps$ and $100ps$ timescales, respectively. In the left panel, the evolution of the largest FLD size is highlighted by an orange trajectory. With decreasing temperature, down to T_{peak}, a clear enhancement in the time variation of FLD sizes is observed. At T_g, a single, large FLD dominates the glass and exhibits minimal fluctuations across the $200ps$ time window.

SUMMARY

In summary, we have employed MD simulations to show that distinct structural features accompany dynamical crossovers in liquid $Cu_{64}Zr_{36}$. Comparing the liquid relaxation time, τ_M, to measures of structure lifetimes, τ_{LC} and $\tau_{icos}^{(FLD)}$, allows us to identify the temperature ranges in which cooperative structural rearrangements contribute to the liquid's relaxation processes. At $T_A \approx 2 \times T_g$ atoms begin to cooperatively form connected icosahedra off of

16

isolated ones, serving as the beginning of the icosahedral ordering that eventually dominates the system. This accompanies the onset of the super Arrhenius growth of η and the break down of the Stokes-Einstein relationship in the liquid.

In the supercooled regime, $T_D \approx 1.4 \times T_g$ marks the early development of stretched glassy dynamics, and the decoupling of Cu and Zr diffusivities. These dynamical features are a manifestation of rapidly growing Zr-rich domains of connected icosahedra, which possess macroscopics numbers of the liquid's icosahedra. Below $925K$ these FLDs stabilize abruptly, and eventually percolate the system before the liquid reaches T_g. Our results provide needed evidence and explanation for the structural roles played at T_A, which according to recent experimental results is an important characteristic temperature for all metallic liquids [14], and more broadly illustrates that a cascade of cooperative structural and dynamical effects begins at this temperature and characterizes the supercooled liquid as it approaches T_g.

---

[1] G.P. Johari and M Goldstein, *Viscous liquids and the glass transition. II. Secondary relaxations in glasses of rigid molecules.* J Chem Phys **55**, 2372-2399 (1970).

[2] C.A. Angell, K.L. Ngai, G.B. McKenna, P.F. McMillan, and S.W. Martin, *Relaxation in glassforming liquids and amorphous solids.* J App Phys **88**, 3113 (2000).

[3] A. Cavagna, *Supercooled liquids for pedestrians.* Phys Rep **476**, 51-124 (2009).

[4] W. Götze, in *Complex Dynamics of Glass-Forming Liquids: A Mode-Coupling Theory.* Oxford University Press (2009).

[5] T.R. Kirkpatrick, D. Thirumalai, and P.G. Wolynes, *Scaling concepts for the dynamics of viscous liquids near an ideal glassy state.* PRA **40**, 1045-1054 (1989).

[6] S. Karmakar, C. Dasgupta, and S. Sastry, *Growing length scales and their relation to timescales in glass-forming liquids.* Annu Rev Condens Matter Phys **5**, 255-284 (2014).

[7] S.A. Kivelson and G. Tarjus, *In search of a theory of supercooled liquids.* Nature Mater **7**, 831-833 (2008).

[8] P.G. Debenedetti and F.H Stillinger, *Supercooled liquids and the glass transition.* Nature **410**, 259-267 (2001).

[9] S.P. Das, *Mode-coupling theory and the glass transition in supercooled liquids.* Rev Mod Phys **76**, 785-851 (2004).

[10] C.A. Angell, *Formation of glasses from liquids and biopolymers.* J Non-Cryst Solids **354**, 4703-4712 (2008).

[11] H. Tanaka, *General view of a liquid-liquid phase transition.* Phys Rev E **62**, 6968-6976 (2000).

[12] E. Aharonov, E. Bouchbinder, H.G.E Hentschel, V. Ilyin, N. Makedonska, I. Procaccia, and N. Schupper, *Direct identification of the glass transition: Growing length scale and the onset of plasticity.* EPL **77**, 56002 (2007)

[13] G. Tarjus, S.A. Kivelson, Z. Nussinov, P. Viot, *The frustration-based approach of supercooled liquids and the glass transition: A review and critical assessment.* J Phys: Condens Matter **17**, R1143-R1182 (2005).

[14] M. Blodgett, T. Egami, Z. Nussinov, and K.F. Kelton, *Unexpected universality in the viscosity of metallic liquids.* arxiv:1407.7558 (2014)

[15] S.P. Chen, T. Egami, and V. Vitek, *Local fluctuations and ordering in liquid and amorphous metals.* Phys Rev B **37** 2440-2449 (1988).

[16] H. Tanaka, T. Kawasaki, H. Shintani, and K. Watanabe, *Critical-like behavior of glass-forming liquids.* Nature Mater **9**, 324-331 (2010).

[17] R.E. Baumer and M.J. Demkowicz, *Glass transition by gelation in a phase separating alloy.* Phys Rev Lett **110**, 145502 (2013).

[18] A. Malins, J. Eggers, C.P. Royall, S.R. Williams, and H. Tanaka, *Identification of long-lived clusters and their link to slow dynamics in a model glass.* J Chem Phys **138**, 12A535 (2013)

[19] D. Kivelson, S.A. Kivelson, X. Zhao, Z. Nussinov, G. Tarjus, *A thermodynamic theory of supercooled liquids.* Physica A **216**, 27-38 (1995)

[20] Z. Nussinov, *Avoided phase transitions and glassy dynamics in a geometrically frustrated systems and non-Abelian theories.* Phys Rev B **69**, 014208 (2004).

[21] T. Iwashita, D.M. Nicholson, T. Egami, *Elementary excitations and crossover phenomena in liquids.* Phys Rev Lett **110**, 205504 (2013)

[22] N.A. Mauro, A.J. Vogt, M.L. Johnson, J.C. Bendert, K.F. Kelton, *Anomalous structural evolution in* $Cu_{50}Zr_{50}$ *glass-forming liquids.* App Phys Lett **103**, 021904 (2013).

[23] N.A. Mauro, M. Blodgett, M.L. Johnson, A.J. Vogt, and K.F. Kelton, *A structural signature of liquid fragility.* Nat Commun **5**, 1-7 (2014).

[24] J.C. Bendert, A.K. Gangopahyay, N.A. Mauro, and K.F. Kelton, *Volume expansion measurements in metallic liquids and their relation to fragility and glass forming ability: An energy landscape interpretation.* PRL **109**, 185901 (2012).

[25] S. Plimpton, J Comp Phys 117, 1-19 (1995). http://lammos.sandia.gov

[26] W.M Brown and Y. Masako, *Implementing Molecular Dynamics on Hybrid High Performance Computers Three-Body Potentials.* Comp Phys Comm **184**, 2785-2793 (2013).

[27] M. S. Daw, and M. I. Baskes, *Embedded-atom method: Derivation and application to impurities, surfaces, and other defects in metals.* Phys. Rev. B **29**, 64436453 (1984).

[28] M.I. Mendelev, M.J. Kramer, R.T. Ott, D.J. Sordelet, D. Yagodin, and P. Popel, *Development of suitable potentials for simulation of liquid and amorphous Cu-Zr alloys.* Phil Mag **11**, 967-987 (2009).

[29] W. Shinoda, M. Shiga, and M. Mikami, *Rapid estimation of elastic constants by molecular dynamics simulation under constant stress.* Phys. Rev. B **69**, 1618 (2004).

[30] C.H. Rycroft, G.S. Grest, J.W. Landry, and M.Z. Bazant, *Analysis of granular flow in a pebble-bed nuclear reactor.* Phys Rev E **74**, 021306 (2006)

[31] A.C.Y. Liu, M.J. Neish, G. Stokol, G.A. Buckley, L.A. Smilie, M.D de Jonge, R.T. Ott, M.J. Kramer, and L. Bourgeois, *Systematic mapping of icosahedral short-range order in a melt-spun* $Zr_{36}Cu_{64}$ *metallic glass.* Phys Rev Lett **110**, 205505 (2013).

[32] Y.Q. Cheng, H.W. Sheng, and E. Ma, *Relationship between structure, dynamics, and mechanical properties in metallic glass-forming alloys.* Phys Rev B **78**, 014207 (2008).

[33] J. Ding, Y.Q. Cheng, and E. Ma, *Full icosahedra dominate local order in* $Cu_{64}Zr_{36}$ *metallic glass and supercooled liquid.* Acta Mater **69**, 343-354 (2014).

[34] H.W. Sheng, W.K. Luo, F.M. Alamgir, J.M. Bai, and E. Ma, *Atomic packing and short-to-*

medium range order in metallic glasses. Nature **439**, 419-425 (2006).

[35] R. Soklaski, Z. Nussinov, Z. Markow, K.F. Kelton, and L. Yang, *Connectivity of icosahedra and a dramatically growing static length scale in Cu-Zr binary metallic glasses.* Phys Rev B **87**, 184203 (2013).

[36] J.P. Hansen and I.R. McDonald, in *Theory of Simple Liquids.* (Academic Print, Amsterdam, 2006). 3rd Edition, 230-234.

[37] A. Inoue, B. Shen, N. Nishiyami, T. Egami, R. S. Aga, J. Morris, Z.P Lu, Y. Liu, C.T. Liu, M.K. Miller et al, in *Bulk Metallic Glasses*, edited by M. Miller and P. Liaw. (Springer, New York, 2008).

[38] J.C. Slater, *Atomic Radii in Crystals.* J. Chem. Phys. **39**, 3199 (1964).

[39] M.T. Cicerone and M.D. Edinger, *Enhanced translation of probe molecules in supercooled o-terphenyl: Signature of spatially heterogeneous dynamics?.* J. Chem. Phys **104**, 7210 (1996).

[40] M.K. Mapes, S.F. Swallen, and M.D. Ediger, *Self-diffusion of supercooled o-terphenyl near the glass transition temperature.* J. Phys. Chem. B **110**, 507511 (2006).

[41] S. Swallen, P. Bonvallet, R. McMahon, and M. Ediger, *Self-Diffusion of tris-Naphthylbenzene near the Glass Transition Temperature.* Phys. Rev. Lett. **90**, 14 (2003).

[42] J. Brillo, A.I. Pommrich, and A. Meyer, *Relation between self-diffusion and viscosity in dense liquids: New experimental results from electrostatic levitation.* Phys. Rev. Lett. **107**, 14 (2011).

[43] J. Brillo, S.M. Chathoth, M.M. Koza, and A. Meyer, *Liquid Al80Cu20: Atomic diffusion and viscosity.* Appl. Phys. Lett. **93**, 14 (2008).

[44] A. Meyer, W. Petry, M. Koza, and M.P. Macht, *Fast diffusion in ZrTiCuNiBe melts.* Appl. Phys. Lett. **83**, 38943896 (2003).

[45] A. Jaiswal, T. Egami, and Y. Zhang, *Atomic-scale dynamics of a model glass-forming metallic liquid: Dynamical crossover, dynamical decoupling, and dynamical clustering.* Phys. Rev. B **91**, 1-14 (2015).

[46] S.W. Basuki, A. Bartsch, F. Yang, K. Rtzke, A. Meyer, and F. Faupel, *Decoupling of Component Diffusion in a Glass-Forming Zr46.75Ti8.25Cu7.5Ni10Be27.5 Melt Far above the Liquidus Temperature.* Phys. Rev. Lett. **113**, 15 (2014).

[47] Y. Zhang, C. Wang, M. Mendelev, F. Zhang, M.J. Kramer, and K.M. Ho, *Diffusion in a Cu-Zr metallic glass studied by microsecond-scale molecular dynamics simulations.* Phys. Rev. B. **91**, 1-5 (2015).

[48] D.B. Miracle, W.S. Sanders, and O.N. Senkov, *The influence of efficient atomic packing on the constitution of metallic glasses.* Philos. Mag. **83**, 24092428 (2003).

[49] Z.W. Wu, M.Z. Li, W.H. Wang, and K.X. Liu, *Correlation between structural relaxation and connectivity of icosahedral clusters in CuZr metallic glass-forming liquids.* Phys Rev B **88**, 054202 (2013).

[50] M. Lee, C. Lee, K. Lee, E. Ma, and J. Lee, *Networked interpenetrating connections of icosahedra: Effects on shear transformations in metallic glass.* Acta Mater **59**, 159-170 (2011)

[51] Y. Zhang, M.I. Mendelev, C.Z. Wang, R. Ott, F. Zhang, M.F. Besser, K.M. Ho, and M.J. Kramer, *Impact deformation on the atomic structure and dynamics of a Cu-Zr metallic glass: A molecular dynamics study.* Phys Rev B **90**. 174101 (2014).

[52] M. Wakeda and Y. Shibutani, *Icosahedral clustering with medium-range order and local elastic properties of amorphous metals.* Acta Mater **58**, 3963-3969 (2010)

[53] Y. Liu, S.L. Ye, B. An, Y.G. Yang, Y.J. Li, L.C. Zhang, and W.M Wang. J. Alloys Compd **587**, 59-65 (2014).

[54] Q. Wang, J.H. Li, J.B. Liu, B.X. Liu, *Effects of mechanical compression and autoclave treatment on the backbone clusters in the $Al_{86}Ni_9La_5$ amorphous alloy.* Phys Chem Chem Phys **16**, 19590-19601 (2014).

[55] J.D. Hunter, Matplotlib: A 2D graphics environment, Comp Sci Eng 9, 90-95 (2007). http://matplotlib.org/